

DOI: 10.1002/cssc.200((will be filled in by the editorial staff))

## TiO<sub>2</sub>(B)/anatase composites synthesized by spray drying as high performance negative electrode material in Li-ion batteries

Edgar Ventosa,<sup>[a]</sup> Bastian Mei,<sup>[b]</sup> Wei Xia,<sup>[b]</sup> Martin Muhler,<sup>[b]</sup> and Wolfgang Schuhmann<sup>[a]</sup>

The successful commercialization of batteries containing Li<sub>4</sub>Ti<sub>5</sub>O<sub>12</sub><sup>[1,2]</sup> is a clear indication that the smaller energy density of titanate-based negative electrodes caused by their high potential of Li-ion storage (1.5-1.8 V vs Li/Li<sup>+</sup>) can be compensated for at least certain applications by their high safety, stability and rate capability. The theoretical Li-ion storage capacity of TiO<sub>2</sub> (335 mAhg<sup>-1</sup>) is twice as that of Li<sub>4</sub>Ti<sub>5</sub>O<sub>12</sub> (175 mAhg<sup>-1</sup>), thus shifting TiO<sub>2</sub> into the spotlight of research interest. The practical capacity of TiO<sub>2</sub>, however, does not reach the theoretical value preventing its commercialization. The electrochemical performance of TiO<sub>2</sub> is limited due to *i*) the sluggish Li-ion diffusivity and *ii*) the poor electrical conductivity. Several approaches to enhance the electrical conductivity of TiO<sub>2</sub> by e.g. carbon<sup>[3]</sup> or RuO<sub>2</sub><sup>[4]</sup> coatings, foreign doping,<sup>[5,6]</sup> frozen native defects<sup>[7]</sup> or wiring by means of carbon nanotube networks,<sup>[8]</sup> and attempts to improve Li-ion diffusion by nanostructuring<sup>[9]</sup> or mesoporosity<sup>[10]</sup> were reported. The crystal phase of TiO<sub>2</sub> strongly influences the Li-ion diffusivity.<sup>[11]</sup> The β-phase of TiO<sub>2</sub> (TiO<sub>2</sub>(B)) has shown extremely fast Li-ion diffusion,<sup>[11,12]</sup> hence exhibiting the highest rate capability reported to date.<sup>[13,14]</sup> The synthesis methods of TiO<sub>2</sub>(B) which are usually more tedious than those of anatase phase can be considered as holdback for its commercial use in Li-ion batteries.

In this communication, we report on the excellent Li-ion storage performance of TiO<sub>2</sub>(B)/anatase composites synthesized by a simple and scalable continuous spray drying process. To the best of our knowledge, the performance of spray-dried TiO<sub>2</sub> as

negative electrode in Li-ion batteries has not been reported before. Due to the presence of the β-phase in the spray-dried TiO<sub>2</sub>, its electrochemical performance is above state-of-the-art,<sup>[3-8]</sup> and only slightly below the best performances of pure and high surface area TiO<sub>2</sub>(B).<sup>[13,14]</sup> Additionally, Nb-doping of TiO<sub>2</sub>, which has been shown to enhance its electrical conductivity<sup>[15]</sup> and to improve its Li-ion storage performance,<sup>[16]</sup> was combined with the spray drying synthesis to further improve the performance of TiO<sub>2</sub>(B)/anatase.

The spray drying synthesis of TiO<sub>2</sub>(B)/anatase was adapted from<sup>[17]</sup> and is described in detail in the experimental section. The calcination temperature was shown to play a key role in the resulting phase composition of the material. The XRD results shown in Figure 1 indicates that pure anatase TiO<sub>2</sub> and TiO<sub>2</sub>(B)/anatase are obtained at 700°C and 600°C, respectively. Calcination temperatures below 600°C were not examined as that is the minimum temperature required for the complete decomposition of the precursor, Figure S1. The samples are referred to as e.g. Nb0-600 for 0 at% Nb calcined at 600°C. Using the XRD data and HighScore from PAnalytical, we roughly estimated a 70/30 ratio of anatase/β-phase in both Nb0\_600 and Nb1\_600. The low amount of β-phase is likely due to the high calcination temperature, which unfortunately cannot be lowered. The BET surface areas of Nb0\_700, Nb0\_600 and Nb1\_600 were 56, 104 and 129 m<sup>2</sup>g<sup>-1</sup>, respectively. The morphology of the samples (S2) is consistent with the BET results.

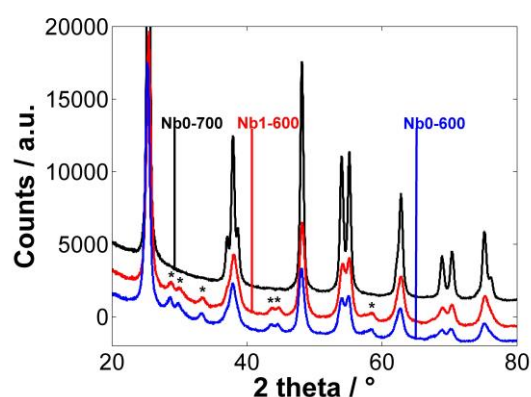


Figure 1. X-ray diffraction patterns of Nb0\_600 (blue line), Nb1\_600 (red line) and Nb0\_700 (black line). Diffraction peaks assigned to TiO<sub>2</sub>(B) are marked with asterisks.

Two mass loadings were investigated for each sample to assess the electrochemical performance at close to particle level (thin films, 1.3 mg cm<sup>-2</sup>) and at film level (thicker films, 4.0 mg cm<sup>-2</sup>) shown in Figures 2a and 2b, respectively. The performance of Nb0\_700 was expected for a nanostructured anatase TiO<sub>2</sub><sup>[18,19]</sup>. Both Nb0\_600 and Nb1\_600 substantially exceeded the performance of Nb0\_700 at all rates, suggesting beneficial effects from the presence of the β-phase. Figure 2c confirmed the presence of electrochemically active β-phase in Nb0\_600 and Nb1\_600 through two plateaus at ca. 1.55 V and 1.60 V (B1 and B2), in addition to the anatase plateau at ca. 1.80 V.<sup>[11]</sup>

[a] Dr. E. Ventosa, Prof. W. Schuhmann  
Analytische Chemie - Elektroanalytik & Sensorik  
Ruhr-Universität Bochum  
Universitätsstr. 150, 44780 Bochum, Germany  
E-mail: edgar.ventosa@rub.de

[b] B. Mei, Dr. W. Xia, Prof. M. Muhler  
Laboratory of Industrial Chemistry  
Ruhr-Universität Bochum  
Universitätsstr. 150, 44780 Bochum, Germany

Supporting information for this article is available on the WWW under <http://www.chemsuschem.org> or from the author. ((Please delete if not appropriate))

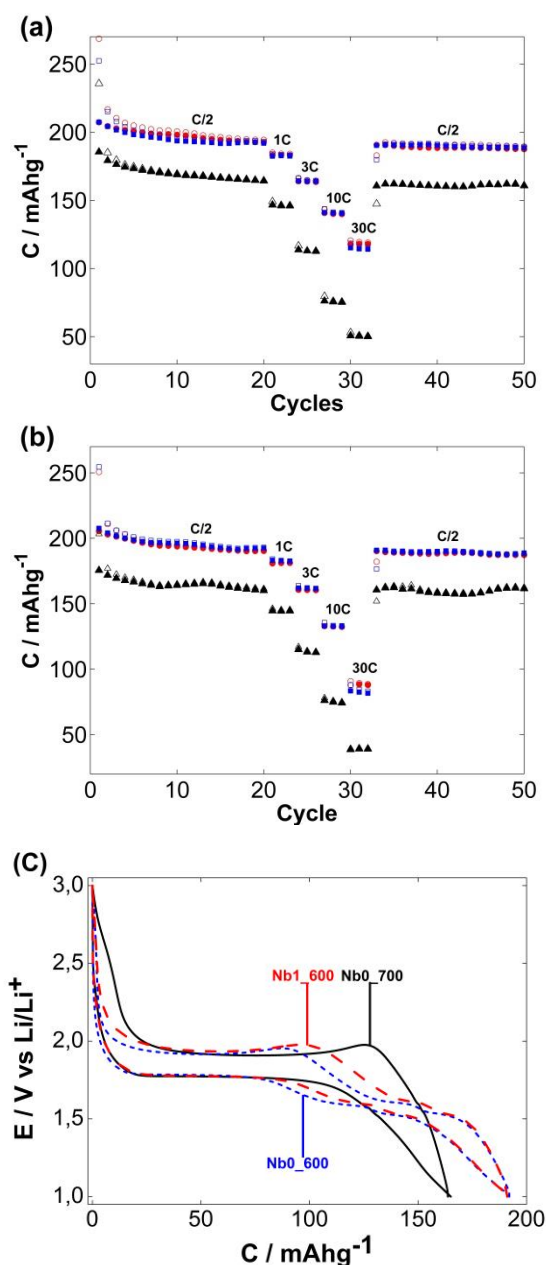


Figure 2. Capacity of intercalation (hollow symbols) and deintercalation (solid symbols) upon cycling for (a) thin electrodes ( $1.3 \text{ mg cm}^{-2}$ ) and (b) thicker electrodes ( $4.0 \text{ mg cm}^{-2}$ ). 20<sup>th</sup> first cycles were carried out at C/2, followed by 1C, 3C, 10C, 30C and C/2. Black triangles for Nb0\_700, blue squares for Nb0\_600 and red circles for Nb1\_600. (c) potential profile for the 20<sup>th</sup> cycle at C/2 of Nb0\_700 (back solid line), Nb0\_600 (blue short dashed line) and Nb1\_600 (red dashed line).

For thin films, the reversible capacity of Nb0\_700 and Nb0\_600 were 165 and 192  $\text{mAhg}^{-1}$ , respectively, after 20 cycles at C/2. The difference in capacity of these two samples became more pronounced with increased rate. At 30C, the reversible capacity of Nb0\_600 is more than twice as that of Nb0\_700 (114 and 50  $\text{mAhg}^{-1}$ , respectively). Although the higher BET surface area of Nb0\_600 might slightly contribute to the improvement,<sup>[19,20]</sup> the presence of  $\text{TiO}_2(\text{B})$ , which is characterized by the presence of more open channels facilitating Li-ion accessibility,<sup>[11,12]</sup> is believed to be mainly responsible. Nb1\_600 showed almost identical performance as Nb0\_600 at low rates, but Nb-doping slightly improved the capacity at 30C by 3% (114 and 118  $\text{mAhg}^{-1}$  for Nb0\_600 and Nb1\_600, respectively). The

retention, which is independent from slight weighting error, also showed a 3% improvement (S3). For higher loadings, no significant changes in capacity were observed at low rates compared to low loadings. At high rates, thin films exceeded the performance of thick films for all samples which indicates that an electric and/or ionic limitation occurs as the thickness of the film increases. As expected, Nb-doping did not show any improvement at low rates, but it did at high rates, as Nb1\_600 exceeded the capacity of Nb0\_600 at 30C by 5% (9% higher in retention, S3)

A detail analysis of the electrochemical data revealed that Nb-doping decreases the resistance of the intercalation-deintercalation process. Figure 3a illustrates the potential separation between intercalation and de-intercalation. Figure 3b, 3c and 3d shows potential separation between intercalation and deintercalation as function of rate, for the plateau of anatase, the first plateau of beta (beta1) and the second plateau of beta (beta2), respectively (more information regarding the calculation of the potential plateau can be found in supporting information). The difference in potential separation increases with increased rate due to the Ohmic drop caused by electric and ionic resistance. For thin film, the overall resistance consists of ionic resistance of the electrolyte, electric and ionic resistance within the particle. The former can be easily estimated by electrochemical impedance spectroscopy (EIS). Values of 7.2 and 5.7 Ohm were obtained for Nb0\_600 and Nb1\_600 (S5), respectively, giving rise to a difference of 1.5 Ohm which accounts only for 30 mV between the two samples at the highest rate (30C). The Li-ion mobility in anatase is sluggish, thus ionic resistance within the particle might have a great contribution in Figure 3b. On the other hand, Li-ion mobility in  $\beta$ -phase is extremely fast,<sup>[11]</sup> thus the smaller potential separation for the Nb-doped sample observed in Figure 3c and 3d is mainly due to enhanced electric conductivity. Additionally, EIS seems to confirm the electric conductivity enhancement, as the middle frequencies semi-circle associated with the electron transfer resistance decreases for Nb1\_600.

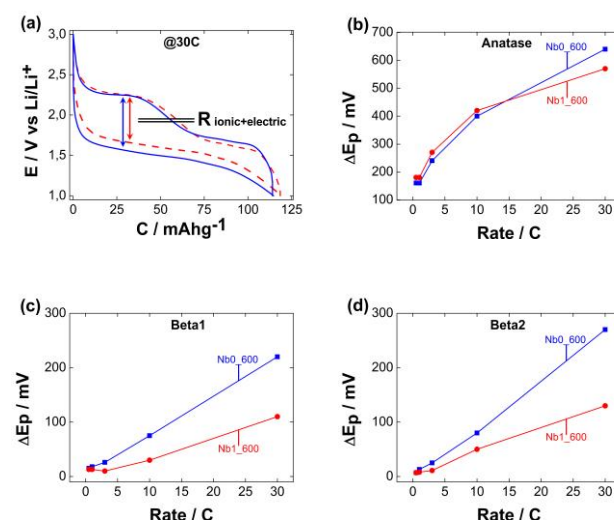


Figure 3. (a) Potential profile curves of Nb0\_600 (blue solid line) and Nb1\_600 (red dotted line) at 30C. (b) Intercalation-deintercalation potential separation as function of rate for (b) the plateau of anatase, (c) the first plateau of  $\beta$ -phase and (d) the second plateau of  $\beta$ -phase.

Shin et al showed recently<sup>[21]</sup> that native doping (oxygen deficiency) has an opposite effect on electric conductivity and Li-

ion mobility, as the former increases and the latter decreases with increased oxygen deficiency. Although further investigation of Nb-doping in simple-phase is required, it seems reasonable that Nb-doping could have a similar opposite effect on TiO<sub>2</sub>. This would explain the limited improvement observed for Nb1\_600 at particle level even at 50C, Figure 4a. Nevertheless, the electric conductivity of the particle is enhanced, which assists in sustaining the electric conductivity through thick films. Figure 4b shows the performance of Nb0\_600 and Nb1\_600 at 40C for 4mg cm<sup>-2</sup>. A current density of ca. 40 mA cm<sup>-2</sup> is applied in these conditions, thus it is not surprising that the capacity of the Nb-doped sample was ca. 30% higher than that of the non-doped one.

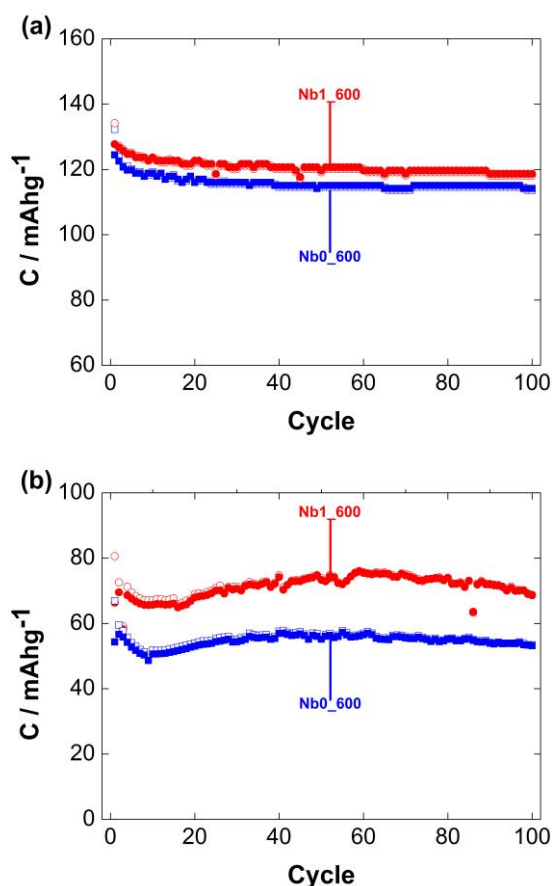


Figure 4. Capacity of intercalation (open symbols) and deintercalation (filled symbols) upon cycling (a) at 50C (100 first cycles) for 1.3 mg cm<sup>-2</sup> and (b) at 40C (100 first cycles) for 4.0 mg cm<sup>-2</sup>. Blue squares for Nb0\_600 and red circles for Nb1\_600. Note that both figures have the same scale: 100 mAhg<sup>-1</sup> x 100 cycles

Efficiencies of 86%, 81% and 82% were obtained in the first cycles at C/2 for Nb0\_700, Nb0\_600, Nb1\_600, respectively. The efficiencies in the second cycles were above 96% in all cases and above 99% by the fifth cycle (S6).

In summary, composites of TiO<sub>2</sub>(B)/anatase nanoparticles synthesized by continuous spray drying showed excellent Li-ion storage performances, especially at high rates, due to the presence of the  $\beta$ -phase. Low mass loading electrodes (1.3 mg cm<sup>-2</sup>) exhibited stable reversible Li-ion storage capacities above 115 mAhg<sup>-1</sup> at 50C (16.8 A g<sup>-1</sup>). Additionally, the synthesis

method is scalable and allows for simultaneous Nb-doping to enhance electrical conductivity. Higher mass loading electrodes (4.0 mg cm<sup>-2</sup>) stored 70 mAhg<sup>-1</sup> at 40C (13.4 A g<sup>-1</sup>), which is 30% higher than that of the analogous non-doped material.

## Experimental Section

TiO<sub>2</sub> nanoparticles were synthesized using a continuous spray drying process adapted as described previously.<sup>[17]</sup> Titanium oxysulfate sulfuric acid hydrate (TiOSO<sub>4</sub> H<sub>2</sub>SO<sub>4</sub> H<sub>2</sub>O, Aldrich) was dissolved in nitric acid solution (1 mol L<sup>-1</sup>) by stirring for at least 4 h. Subsequently, a predetermined amount of ammonium niobate (V) oxalate hydrate ((NH<sub>4</sub>)NbO(C<sub>2</sub>O<sub>4</sub>)<sub>2</sub> H<sub>2</sub>O, Aldrich) was added to the colorless solution to achieve a Nb concentration of 1 at% relative to Ti. The solution was stirred for 1 h and used for the synthesis of Nb-doped TiO<sub>2</sub> precursor materials through a continuous spray drying method. A bench-top spray dryer (B-290, Büchi) with a two-fluid nozzle was used for fast evaporation of the fluid.<sup>[22-24]</sup> The colorless powder samples were collected from the dryer and calcined under flowing synthetic air (20.5% O<sub>2</sub> in He, 100 sccm) at 600°C or 700°C for 1 h. A heating rate of 1 K min was applied leaving sufficient time for flushing out volatile species evolving during the decomposition of the precursors. After calcination the samples were thoroughly washed with distilled water and dried in static air for 24 h at 110°C.

Electrochemical experiments were carried out using three-electrodes Swagelok-type cells assembled in an argon-filled glove box. The working electrodes were prepared by the "Doctor-Blade" technique and consisted of the active material (TiO<sub>2</sub>), a conductive additive (C65 carbon black, Timcal, Bodio, Switzerland) and a binder (poly-vinylidene difluoride, Solef S5130, Solvay) in a weight ratio of 76:15:9, pasted on a 12 mm Cu disc. Two mass loadings were evaluated for each sample using about 1.3 and ca. 4.0 mg cm<sup>-2</sup>. Glass fiber (WhatmanGF/D) filters soaked in LP40 electrolyte (Merck, Darmstadt, Germany) were used as separators. Lithium foil was used as counter electrode and reference electrode. Galvanostatic cycling of the assembled cells was carried out using a Bio-Logic VMP-3 (Bio-Logic SAS, Claix, France) in the potential range of 1.0-3.0V at different current densities (1C is equivalent to 336 mA g<sup>-1</sup>). All potentials are reported versus the Li/Li<sup>+</sup> potential.

## Acknowledgements

Financial support by the EU and the state NRW in the framework of the HighTech.NRW program for funding of CES, the DFG in the framework of SPP 1473 (WeNDeLIB; SCHU 929/11-1) and the Ruhr-University Research School is gratefully acknowledged.

**Keywords:** Li-ion batteries · high C-rate ·  $\beta$ -TiO<sub>2</sub> · Nb doping · spray drying

- [1] A. Du Pasquier, C. C. Huang, T. Spittler, *J. Power Sources* **2009**, *186*, 508
- [2] T. Tan, H. Yumoto, D. Buck, B. Fattig, C. Hartzog, *The World Electric Vehicle Journal* **2007**, *2*, 76
- [3] F.-F. Cao, X.-L. Wu, S. Xin, Y.-G. Guo, L.-J. Wan, *J. Phys. Chem. C* **2012**, *114*, 10308
- [4] Y.-G. Guo, Y.-S. Hu, W. Sigle, J. Maier, *Adv. Mater.* **2007**, *19*, 2087
- [5] L. Aldon, P. Kubiak, A. Picard, J.C. Jumas, and J. Olivier-Fourcade, *Chem. Mater.* **2006**, *18*, 1401
- [6] M. V. Koudriachova, N. M. Harrison, *J. Mater. Chem.* **2006**, *16*, 1973
- [7] J.-Y. Shin, J. H. Joo, D. Samuliel, J. Maier, *Chem. Mater.* **2012**, *24*, 543
- [8] E. Ventosa, P. Chen, W. Schuhmann, W. Xia, *Electrochem. Commun.* **2012**, *25*, 132
- [9] A. S. Arico, P. G. Bruce, B. Scrosati, J. M. Tarascon, W. V. Schalkwijk, *Nat. Mater.* **2005**, *4*, 366

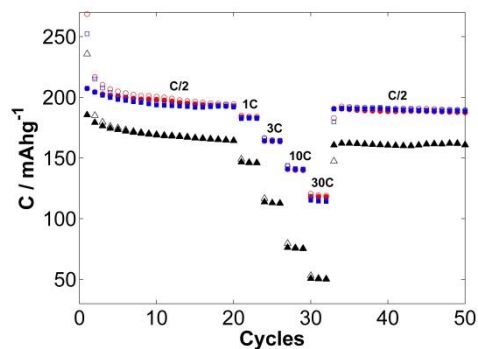
- [10] K. Saravanan, K. Ananthanarayanan, P. Balaya, *Energy Environ. Sci.* **2010**, *3*, 939
- [11] M. Zúkalová, M. Kalbac, L. Kavan, I. Exnar, M. Graetzel, *Chem. Mater.* **2005**, *17*, 1248
- [12] A. R. Armstrong, G. Armstrong, J. Canales, P. G. Bruce, *Angew. Chem. Int. Ed.* **2004**, *43*, 2286
- [13] Y. Ren, Z. Liu, F. Pourpoint, A. R. Armstrong, C. P. Grey, P. G. Bruce, *Angew. Chem. Int. Ed.* **2012**, *51*, 2164
- [14] S. Liu, H. Jia, L. Han, J. Wang, P. Gao, D. Xu, J. Yang, S. Che, *Adv. Mater.* **2012**, *24*, 3201
- [15] S. X. Zhang, D. C. Kundaliya, W. Yu, S. Dhar, S. Y. Young, L.G. Salamanca-Riba, S. B. Ogale, R. D. Vispute, T. Venkatesan, *J. Appl. Phys.* **2007**, *102*, 013701
- [16] Y. Wang, B. M. Smarsly, I. Djerdj, *Chem. Mater.* **2010**, *22*, 6624
- [17] B. Mei, M. D. Sánchez, T. Reinecke, S. Kaluza, W. Xia, M. Muhler, *J. Mater. Chem.* **2011**, *21*, 11781
- [18] G. Sudant, E. Baudrin, D. Larcher, J. M. Tarascon, *J. Mater. Chem.* **2005**, *15*, 1263.
- [19] C. Jiang, M. Wei, Z. Qi, T. Kudo, I. Honma, H. Zhou, *J. Power Sources* **2007**, *166*, 239.
- [20] M. Wagemaker, W. J. H. Borghols, F. M. Mulder *J. Am. Chem. Soc.* **2007**, *129*, 4323
- [21] J.-Y. Shin, J. H. Joo, D. Samuelis, J. Maier, *Chem. Mater.*, **2012**, *24*, 543
- [22] S. Kaluza, M. K. Schröter, R. Naumann d'Alnoncourt, T. Reinecke, M. Muhler, *Adv. Funct. Mater.* **2008**, *18*, 3670
- [23] S. Kaluza, M. Muhler, *Mater. Chem.* **2009**, *19*, 3914
- [24] S. Kaluza, M. Muhler, *Catal. Lett.* **2009**, *129*, 287
- 

Received: ((will be filled in by the editorial staff))

Published online: ((will be filled in by the editorial staff))

## COMMUNICATION

**The power of spray-dried TiO<sub>2</sub> in LIBs:** TiO<sub>2</sub>(B)/anatase synthesized by spray drying exhibits excellent Li-ion storage performances, exceeding 115 mAhg<sup>-1</sup> at 16.8 Ag<sup>-1</sup> (50C). The scalable synthesis method also allows for Nb-doping, which assists in sustaining electric conductivity as the thickness of film increases.



*Edgar Ventosa,<sup>[a]</sup> Bastian Mei,<sup>[b]</sup>  
Wei Xia,<sup>[b]</sup> Martin Muhler,<sup>[b]</sup> and  
Wolfgang Schuhmann<sup>[a]</sup>*

**Page No. – Page No.**

**TiO<sub>2</sub>(B)/anatase composites  
synthesized by spray drying as  
high performance negative  
electrode material in Li-ion  
batteries**

## Supporting Information.

### TiO<sub>2</sub>(B)/anatase synthesized by spray drying as high performance negative electrode material in Li-ion batteries

Edgar Ventosa,<sup>[a]\*</sup> Bastian Mei,<sup>[b]</sup> Wei Xia,<sup>[b]</sup> Martin Muhler,<sup>[b]</sup> and Wolfgang Schuhmann<sup>[a]</sup>

Thermogravimetry (Cahn TG 2131 thermobalance) was used to evaluate the decomposition of the TiOSO<sub>4</sub> precursor. The sample was heated with 1 K min<sup>-1</sup> resulting in the decomposition profile shown in Figure S1. The decomposition profile consists of three main regions. The two regions in the temperature range from 50°C to 250°C with an overall weight loss of 20% are likely due to the release of water as previously reported by Mei et al.<sup>[1]</sup> The main weight loss, however, is observed for temperatures above 500°C. This weight loss is related to the decomposition of the precursors sulfur compounds.<sup>[1]</sup> Therefore, minimum calcination temperature of around 600°C is required to fully decompose the precursor and remove all synthesis residues.

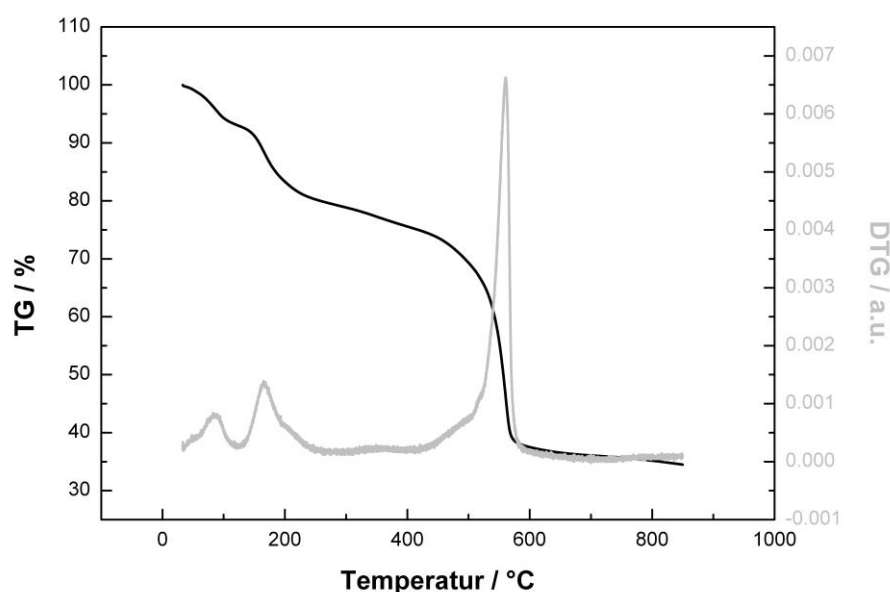
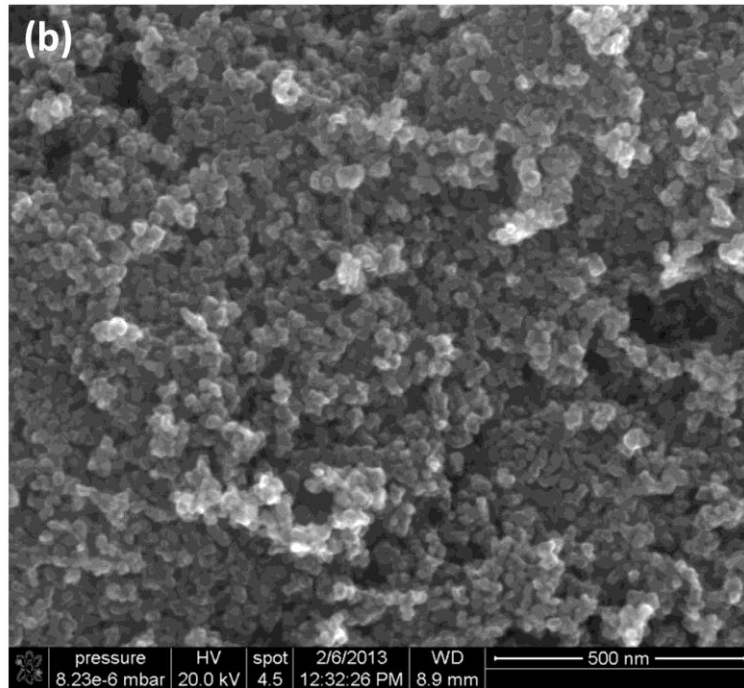
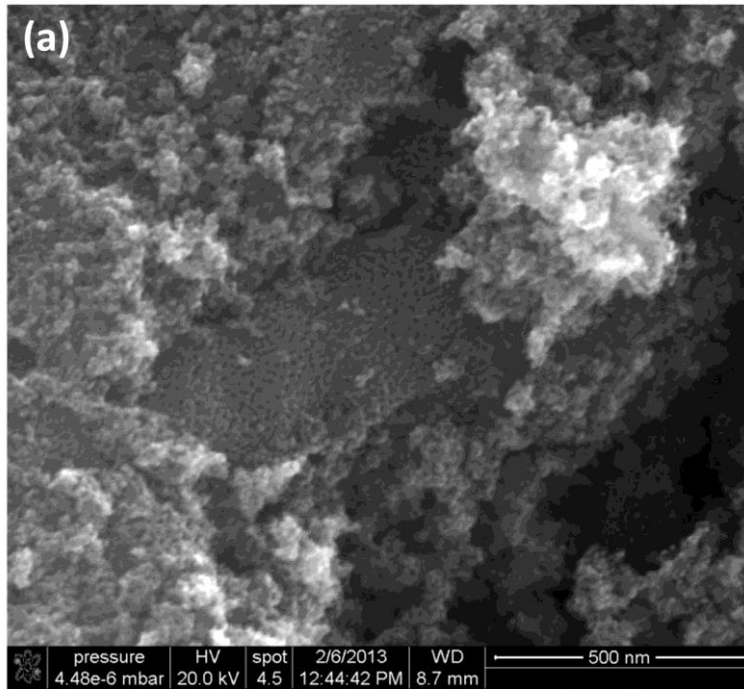


Figure S1. TG and DTG curves of TiOSO<sub>4</sub> precursor.

The morphology of the three samples was characterized by scanning electron microscopy, Dual Beam<sup>TM</sup> 3D FEG, as shown in Figure S2. The morphology of Nb0\_600 and Nb1\_600 is similar to each other, whereas Nb0\_600 reveals a morphology featured by larger particles. Hence, the morphology of the samples is consistent with the results of BET surface areas.



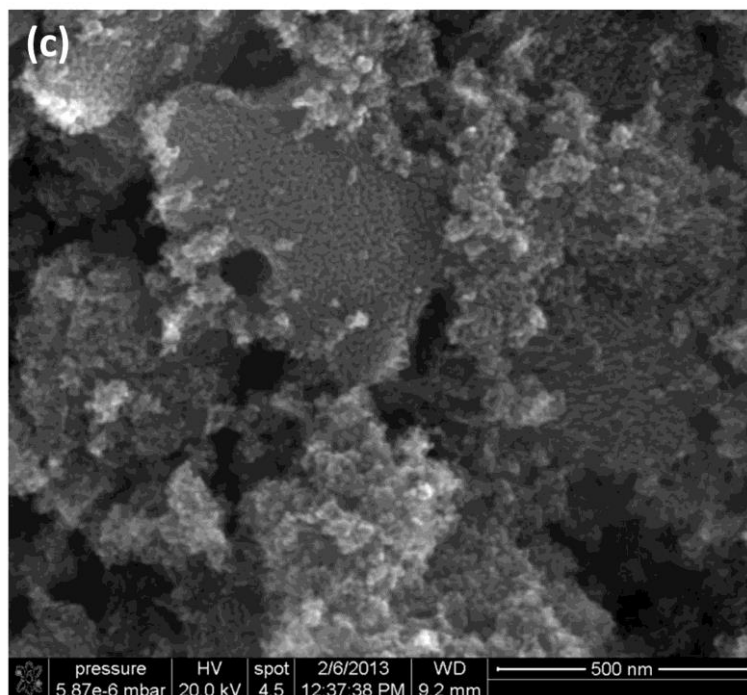


Figure S2. SEM images of (a) Nb0\_600, (b) Nb0\_700 and (c) Nb1\_600.

The evaluation of rate capability of materials for Li-ion batteries based on their capacities given in  $\text{mAhg}^{-1}$  can be influenced by weighing errors, especially at high rates and low loadings, while the retention is not. To ensure that the performances of the samples observed at high rates are due to their rate capability and not to errors in weighing, we compare the retentions as well. Figure S3 shows the retention of Nb0\_600 and Nb1\_600 for (a) 1.3 and (b) 4.0  $\text{mg cm}^{-2}$ . In retention, doped-sample also exhibited improved performance at 30C, following the same trend as the capacity comparison.

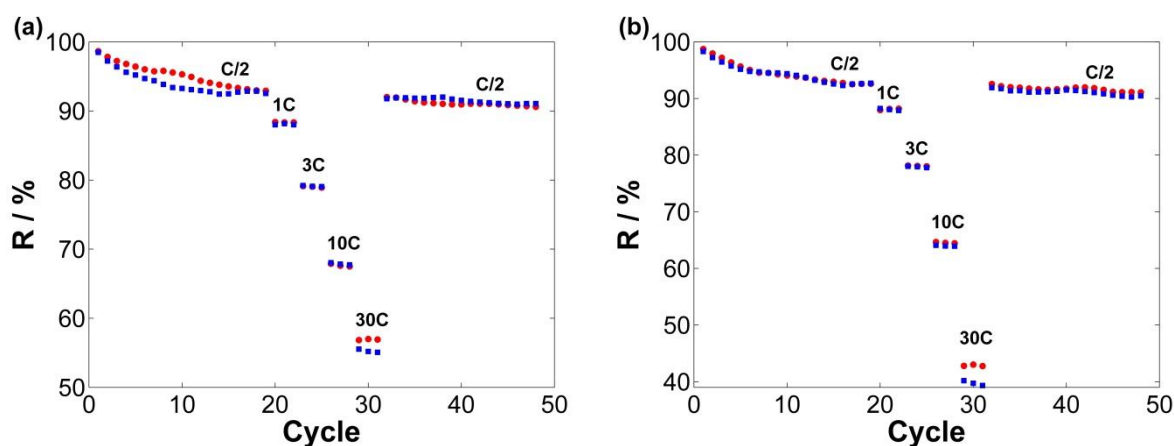


Figure S3. Reversible capacity retention of Nb0\_600 (blue squares) and Nb1\_600 (red circles) upon cycles for mass loading of (a) 1.3  $\text{mgcm}^{-2}$  and (b) 4.0  $\text{mgcm}^{-2}$

The estimation of the intercalation/deintercalation potentials directly from the chronopotentiometry transients becomes more difficult at high rates as the plateaus become sloppier. The differential of potential versus capacity is calculated and the inverse of such differential is plotted against potential.

Such plot is often called differential capacity. An example of potential – capacity profile and its differential capacity – potential is shown in Figure S4. The peaks in the differential capacity – potential represent the plateaus in the potential – capacity profiles. Consequently, the potential of each plateau can be estimated precisely even at 30C.

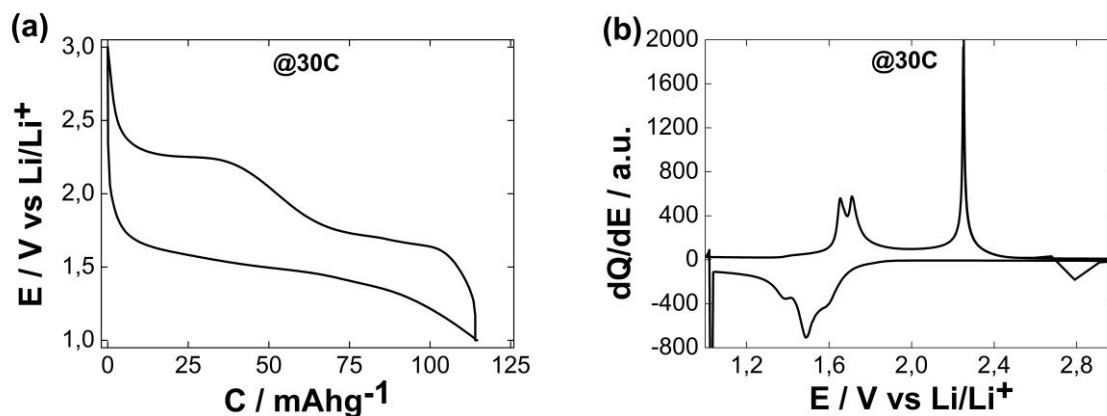


Figure S4. (a) Potential – capacity profile and (b) differential capacity ( $dQ/dE$ ) – potential of Nb0\_600 at 30C for a film loading of  $1.3 \text{ mg cm}^{-2}$

Electrochemical impedance spectroscopy was performed in the frequency range 100 KHz - 100 mHz. The objective of this technique is to determine the ionic resistance of the electrolyte and the electron transfer resistance of the material. The impedance spectra of Nb0\_600 and Nb1\_600 are shown in Figure S5. The resistances of the electrolyte were 7.2 and 5.7 Ohms for Nb0\_600 and Nb1\_600, respectively. As for the electron transfer resistance, a decrease in the size of the semi-circle from non-doped to Nb-doped samples is observed. Although the electron transfer resistance results are not to be overinterpreted as the value for non-doped  $TiO_2$  is already small and thus it might be sensitive to misalignment or scaling errors, EIS spectra indicate that doping decreases the electron transfer resistance which is consistent with Figure 2 of the manuscript.

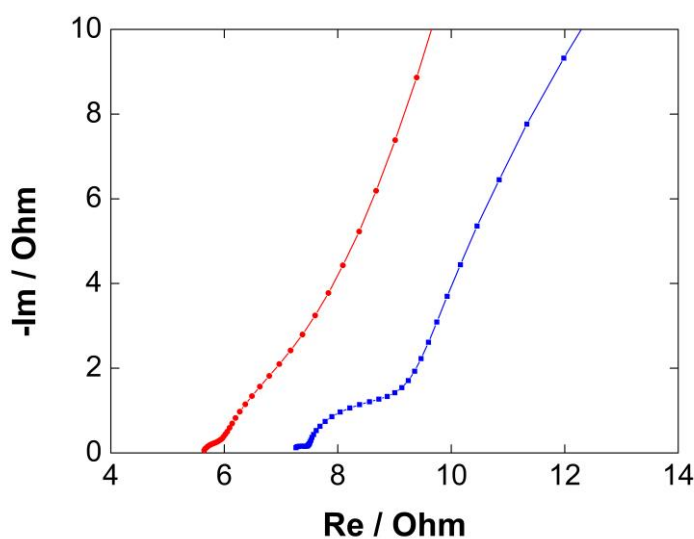


Figure S5. EIS spectra of Nb0\_600 (blue squares) and Nb1\_600 (red circles).

Efficiency of the intercalation and deintercalation process, which represents the percentage of total charge that is reversibly stored, is an important parameter of any active materials in batteries. Therefore we report in Figure S6 the efficiency of Nb0\_70, Nb0\_600 and Nb1\_600 upon the first 50 cycles for mass loading of ca.  $4.0 \text{ mg cm}^{-2}$ . Efficiencies of 86%, 81% and 82% were obtained in the first cycles at C/2 for Nb0\_700, Nb0\_600, Nb1\_600, respectively. The efficiencies in the second cycles were above 96% in all cases and above 99% by the fifth cycle.

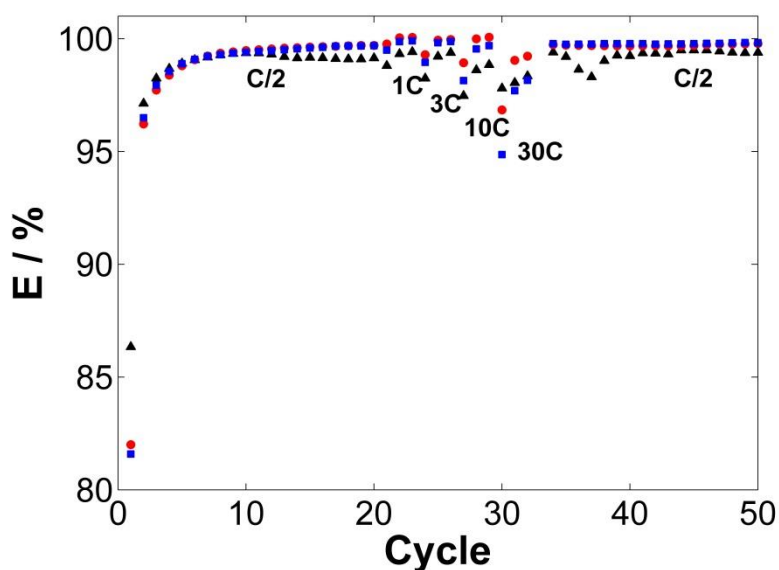


Figure S6. Efficiencies of Nb0\_700 (black triangles), Nb0\_600 (blue squares) and Nb1\_600 (red circles) upon cycles for mass loading of ca.  $4.0 \text{ mg cm}^{-2}$ .

- [1] B. Mei, M. D. Sánchez, T. Reinecke, S. Kaluza, W. Xia, M. Muhler, *J. Mater. Chem.* **2011**, *21*, 11781

## Accompanying letter

“TiO<sub>2</sub>(B)/anatase synthesized by spray drying as high performance negative electrode material in Li-ion batteries” by E. Ventosa, B. Mei, W. Xia, M. Muhler, W. Schuhmann

In the initially submitted manuscript, a key issue raised by both referees was a request for an in-depth discussion of the effects of Nb-doping on the electrochemical performance of TiO<sub>2</sub>. We substantially improved this aspect in the revised version. Moreover, we emphasized more on the idea of spray-drying synthesis of TiO<sub>2</sub> as a simple and scalable method to produce TiO<sub>2</sub> which shows performance above the state of the art of TiO<sub>2</sub> based negative electrode material in Li-ion batteries (LIBs). We have addressed the questions of the referees as shown in detail below.

Major changes are related to 6 new figures in the main text (Figure 1c, 3a, 3b, 3c, 3d and 4a) and 4 more new figures in the supporting information (Figures S1, S4a, S4b and S5) in the new revised manuscript. Modifications in the text were highlighted in yellow. In addition, in order to be more precise, we have slightly changed the title in order to put more gravity to the main idea of the manuscript, which is seen in the excellent performance of TiO<sub>2</sub> synthesized by spray-drying as negative electrode material in LIBs. We are convinced that the performance of the newly proposed material is remarkable, with a stable reversible capacity of above 120 mAhg<sup>-1</sup> at 50C (16.8 A g<sup>-1</sup>) which is only slightly below the best performance reported to date (Angew. Chem. Int. Ed. 2012, 51, 2164; Adv. Mater. 2012, 24, 3201), however, using the advantages of spray-drying as synthesis method, i.e. simple, quick and scalable.

We want to express our acknowledgements to the referees who have kindly taken their time to review our manuscript.

(Dr. Edgar Ventosa)

---

**Referee1.** This paper reported Nb-doped TiO<sub>2</sub>(B)/anatase composites synthesized by spray drying as Li-ion batteries negative electrode material. The highlight of this paper may be the high discharge capacity. However, the high discharge capacity may be due to the thin active material layer synthesized by the spray drying method. This article is not new. I think that this article may be more suitable for Journal of Power Sources, ElectrochimicaActa, Solid State Ionics and Journal of the Electrochemical Society.

**Reply.** Obviously there is a misunderstanding in the overall synthesis of the electrode. Spray drying is yielding a powder, which is then further processed by addition of a carbon black and binder and finalized by using doctor blading. Thus, spray drying is not connected with the finally obtained film thickness. The film thickness was standard for high-rate charge/discharge experiments (about 1 mg cm<sup>-2</sup>). Unlike batteries used in applications (such as cars) the film was thin enough to avoid diffusional limitations in the liquid at high rate. This enables us to in-depth evaluate the materials properties. Similar loadings can be found in a large number of articles such as *Chem. Mater.* 2012, 24, 543; *Angew.Chem. Int. Ed.* 2010, 49, 2570; *Adv. Mater.* 2012, 24, 3201.

**Referee 1.** In fact, this synthesized method is not new, and it has been used as the synthesis of other electrode material (such as LiMn<sub>2</sub>O<sub>4</sub>).

**Reply.** Spray drying was to the best of our knowledge not used before to synthesize TiO<sub>2</sub> for Li-ion batteries. Spray drying is evidently a mature technique, which was for the first time used for TiO<sub>2</sub> synthesis for LIBs. This is evidently of high importance due to the fact that while keeping the quality of the primarily synthesized material spray drying has an option for up-scaling.

**Referee1.** Compared with other paper on TiO<sub>2</sub>, there is no novelty. The author can not report that why the Nb doping can improve the electrochemical performance of TiO<sub>2</sub>. Hence, the author should give the effect of Nb doping on structure and electrochemical kinetic of TiO<sub>2</sub>.

**Reply.** Despite the proposed synthesis is already novel we agree with the referee that the effect of Nb-doping was not discussed to the necessary depth in the first submission of the manuscript. We included additional results and discussion to address this point (second and third paragraph on page 2 and Figure 3)

**Referee1.** The author confirm that the theoretical Li-ion storage capacity of TiO<sub>2</sub> (335mAhg<sup>-1</sup>) is twice as that of Li<sub>4</sub>Ti<sub>5</sub>O<sub>12</sub> (175 mAhg<sup>-1</sup>). In fact, the reversible capacity of Li<sub>4</sub>Ti<sub>5</sub>O<sub>12</sub> discharged to 0 V can reach 230 mAhg<sup>-1</sup>. Please see DrYi<sub>4</sub>sreport(Journal of Power Sources 214 (2012) 220;Journal of Power Sources 215 (2012) 258; Journal of Power Sources 222 (2013) 448.)

**Reply.** One of the main advantages of TiO<sub>2</sub> based negative electrode materials in LIBs is seen in avoiding massive formation of the Solid Electrolyte Interphase (SEI) by operating above it at 1.0 V. We deliberately discussed the properties of this material exclusively in the stability window of the electrolyte which is seen as one of the key advantages of TiO<sub>2</sub> based electrodes especially with respect to safety considerations. The theoretical capacity of TiO<sub>2</sub> within this stability window is

larger than that of  $\text{Li}_4\text{Ti}_5\text{O}_{12}$ . Similar statements can be found in [*Angew. Chem. Int. Ed.* 2012, 51, 2164; *Adv. Energy Mater.* 2012, 2, 322; *Chem. Mater.* 2012, 24, 4468]

---

**Referee 2.** This is an interesting article and gives a new dimension for developing innovative anode materials for Li-ion batteries. Especially comparison of storage performances for low and high loading is interesting. The manuscript is acceptable; however this reviewer feels that some revision is required addressing following questions:

**Referee 2.** Why did authors select to dope only with 1% of Nb, why not higher concentration, some justification is required.

**Reply.** We have chosen this amount of doping as an exemplary amount of doping chosen in order to provide evidence for a proof of concept. Despite conductivity is best at 6% Nb doping, the doping level was chosen based on the findings by Shin et al (*Chem. Mater.* 2012, 24, 543) who reported that the introduction of oxygen deficiency is beneficial for the electrochemical performance of  $\text{TiO}_2$ . Oxygen vacancies enhance the electric conductivity but decrease the Li-ion mobility due to defects. These are contradictory effects which suggested that a low doping level would be most beneficial for this specific application. Additionally, doping levels of as high as 5-10% might lead to the formation of  $\text{Nb}_2\text{O}_5$  islands.

**Referee 2.** How do authors control doping of Nb into  $\text{TiO}_2$  (B) phase rather than anatase phase? Why not providing some structural data with refinement if possible to discuss the volume changes to guess the doped site/phase.

**Reply.** Controlling the doping in one phase over another can hardly be achieved by this method. We did introduce in the new manuscript an approach (page 2) that shows the Nb-doping has beneficial effect on the electrochemical performance of both phases.

**Referee 2.** What is the ratio of the  $\text{TiO}_2$  (B) and anatase and how do authors control this ratio, I do not see any systematic synthesis attempt to control on such parameter.

**Reply.** The ratio has been estimated from XRD data to be 30% (B)/70 anatase (third paragraph; page 1). The electrochemical results are consistent with that value. We controlled this ratio by the temperature of the calcination, 30/70 and 0/100 for 600°C and 700°C, respectively. Lower temperatures will likely lead to higher amounts of B-phase, as B-phase starts to be transformed into anatase at temperatures as low as 350°C. Since the residues on the surface of  $\text{TiO}_2$  require 600°C to be removed. Massive reduction of these residues, which lead to electrochemical failure upon cycling, is observed at calcination temperature of 500°C. We believe that a systematic attempt to control such parameter could be an interesting full paper to follow up this communication.

**Referee 2.** Since the analysis is mostly related to improved conductivity due to doping, it would be beneficial to provide some impedance data reflecting changes associated with charge transport/ transfer resistances.

**Reply.** We agree with the referee. We have changed the manuscript accordingly and integrated both impedance analysis together with a novel approach to distinguish the contribution of Nb-doping in the electrochemical response.